Synthesis, Structure, and Redox Properties of a New Aqua Ruthenium Complex Containing the Tridentate [9]aneS$_3$ and the Didentate 1,10-Phenanthroline Ligands

Xavier Sala,[a] Albert Poater,[a] Isabel Romero,[a] Montserrat Rodríguez,[a] Antoni Llobet,*[a] Xavier Solans,[b] Teodor Parella,[c] and Teresa M. Santos[d]

Keywords: Thioether compounds / Catalysis / Oxidations / Redox chemistry / Ruthenium

The synthesis of a new Ru–H_2O complex [Ru(phen)(H_2O)([9]aneS$_3$)](ClO_4)$_2$, **2**, (phen = 1,10-phenanthroline, [9]aneS$_3$ = 1,4,7-trithiacyclononane) is described. The complex is characterized by UV/Vis and 1-D and 2-D NMR spectroscopy in solution. The complex has been further characterized in the solid-state by X-ray diffraction analysis which displays a distorted octahedral coordination geometry around the Ru metal center. The cyclic voltammetric experiments of the complex show a pH-dependent chemically irreversible wave at $E_{p,a}$ = 0.82 V, at pH = 7.0, indicating the low stability of the higher oxidation states. Nevertheless, before the complex decomposes, it is capable of electrocatalytically oxidizing benzyl alcohol (BzOH) to benzaldehyde with a second-order rate constant of 19.8 $M^{-1}s^{-1}$.

Introduction

Over the last two decades a large number of ruthenium polypyridyl complexes containing a water molecule directly bonded to the metal has emerged.[1] The [Ru(trpy)(bpy)(H_2O)]$^{2+}$ (trpy = 2,2′:6′,2′′-terpyridine and bpy = 2,2′-bipyridine) complex described by Meyer et al.[1a] constitutes a paradigm of this type of complexes, both from a structural and a reactivity point of view.

The Ru^{II}–H_2O complexes are of interest since the corresponding higher oxidation states can be reached within a relatively narrow potential range by sequential electron and proton loss, as shown in Equations (1) and (2) for [Ru(trpy)(bpy)(H_2O)]$^{2+}$.

$$[Ru^{II}(trpy)(bpy)(H_2O)]^{2+} \underset{+1H^+,+1e^-}{\overset{-1H^+,-1e^-}{\rightleftharpoons}} [Ru^{III}(trpy)(bpy)(OH)]^{2+} \quad (1)$$

$$E_{1/2}(Ru^{III/II} \text{ at pH} = 7) = 0.49 \text{ V vs. SSCE}$$

$$[Ru^{III}(trpy)(bpy)(OH)]^{2+} \underset{+1H^+,+1e^-}{\overset{-1H^+,-1e^-}{\rightleftharpoons}} [Ru^{IV}(trpy)(bpy)(O)]^{2+} \quad (2)$$

$$E_{1/2}(Ru^{IV/III} \text{ at pH} = 7) = 0.62 \text{ V vs. SSCE}$$

These higher oxidation states, especially Ru^{IV}=O, are active catalysts for a variety of oxidative reactions such as the oxidation of alkenes to epoxides,[2] sulfides to sulfoxides,[3] phosphane to phosphane oxides,[4] alcohols to aldehydes,[5] and even saturated alkanes to alcohols.[6] Furthermore, from a bioinorganic perspective, they have also been shown to be able to selectively bind and cleave DNA molecules.[7]

A challenging aspect associated with the chemistry of Ru–H_2O type of complexes is the understanding of how electronic factors transmitted by the ligands can influence the stability of the different oxidation states, and as a consequence its reactivity.[8] With this purpose several Ru–H_2O complexes have been described containing electron-donating and electron-withdrawing substituents in the polypyridylic ligands,[9] as well those that have a variety of ancillary ligands containing oxygen donors such as picolinate or acetylacetonate and phosphorus donors such as phosphanes.[10]

In this paper we report on the synthesis, structural and spectroscopic characterization of the first example of a Ru–H_2O polypyridylic complex containing a thioether type ligand, [Ru(phen)(H_2O)([9]aneS$_3$)]$^{2+}$ (phen = 1,10-phen-

[a] Departament de Química, Universitat de Girona, Campus de Montilivi, 17071 Girona, Spain
E-mail: antoni.llobet@udg.es
[b] Departament de Cristallografia, Mineralogia i Dipòsits Minerals, Universitat de Barcelona, Martí i Franquès, s/n, 08028 Barcelona, Spain
[c] Departament de Química, Universitat Autònoma de Barcelona, Bellaterra, 08193 Barcelona, Spain
[d] Department of Chemistry, University of Aveiro, 3810–193 Aveiro, Portugal
Supporting information for this article is available on the WWW under http://www.eurjic.org or from the author.

  DOI: 10.1002/ejic.200300137

anthroline. [9]aneS$_3$ = 1,4,7-trithiacyclononane). The electronic properties exerted by the thioether ligand to the metal center are discussed, together with its influence on the redox and catalytic properties.

Results and Discussion

Synthesis and Solid-State Structure

The synthesis of the complex [Ru(phen)(H$_2$O)([9]aneS$_3$)](ClO$_4$)$_2$ (**2**) is straight forward and consists of the addition of Ag^{I} to the corresponding Ru^{II}−Cl complex according to Equation (3).

$$[Ru(Cl)(phen)([9]aneS_3)]^+ + Ag^+ + H_2O \longrightarrow [Ru(phen)(H_2O)([9]aneS_3)]^{2+} + AgCl \quad (3)$$

The crystal structure of complex **2·2H$_2$O** was solved by means of single-crystal X-ray diffraction analysis and its crystallographic data, as well as selected bond lengths and angles are presented in Table 1 and Table 2, respectively. Figure 1 presents the ORTEP diagram for the cationic moiety of the molecule, including the corresponding labeling scheme.

The molecular structure of **2** shows that the Ru metal center has a distorted octahedral coordination environment. The [9]aneS$_3$ ligand coordinates facially through its sulfur atoms in an endodentate manner, while the phen ligand is chelated through its N atoms. The sixth coordination site is occupied by the oxygen atom of the aqua ligand. Bond lengths and angles are within the expected values for this type of complexes.[11,12] It is interesting to note here that the Ru−S bond lengths *trans* to the N atoms of the phen ligand are about 4 pm larger than the Ru−S distance *trans* to the aqua ligand, denoting the stronger *trans* effect of the former ligand with respect to the latter. The S−Ru−S *cis* angles are close to 90° indicating the good facial fit of the ligand for an octahedral type of geometry

Table 1. Crystal data for complex **2**

	2·2H$_2$O
Empirical formula	$C_{18}H_{26}Cl_2N_2O_{11}RuS_3$
Molecular mass	714.56
Crystal system, space group	triclinic, $P\bar{1}$
a, Å	8.143(3)
b, Å	9.137(8
c, Å	18.754(7)
α,°	99.46(5)
β,°	91.52(3)
γ,°	107.77(5)
V, Å^3	1306.3(13)
Formula units per cell	2
Temperature, K	298(2)
λ, Mo-K_α, Å	0.71073
$\rho_{calcd.}$, g cm^{-3}	1.817
μ, mm^{-1}	1.104
R_1[a]	0.0386
wR_2[b]	0.0580

[a] $R_1 = \Sigma F_o - F_c / \Sigma F_o$. [b] $wR_2 = [\Sigma\{w(F_o^2 - F_c^2)^2\}/\Sigma\{w(F_o^2)^2\}]^{1/2}$, where $w = 1/[\sigma^2(F_o^2) + (0.0042P)^2]$ and $P = (F_o^2 + 2F_c^2)/3$.

Table 2. Selected bond lengths [Å] and angles [°] for complex **2**

Ru1−N1	2.086(4)	N1−Ru1−N12	78.08(15)	O1−Ru1−S1	91.03(10)
Ru1−N12	2.101(4)	N1−Ru1−O1	85.97(14)	S2−Ru1−S1	88.61(6)
Ru1−O1	2.183(3)	N12−Ru1−O1	83.78(13)	N1−Ru1−S3	174.20(11)
Ru1−S2	2.2636(18)	N1−Ru1−S2	91.67(11)	N12−Ru1−S3	96.16(12)
Ru1−S1	2.2986(17)	N12−Ru1−S2	96.41(11)	O1−Ru1−S3	94.21(10)
Ru1−S3	2.300(2)	O1−Ru1−S2	177.54(10)	S2−Ru1−S3	88.21(7)
		N1−Ru1−S1	97.84(12)	S1−Ru1−S3	87.95(7)
		N12−Ru1−S1	173.59(12)		

Table 3. pK_a and Electrochemical data at pH = 7.0 in μ = 0.1 phosphate buffer solution or in acetonitrile for related Ru complexes

Complex[a][b]	$E_{1/2}$[c] (IV/III)	$E_{1/2}$[c] (III/II)	pK_a(II)	Ref.	Complex[d]	$E_{1/2}$[b] (III/II)	Ref.
[Ru^{II}(acac)(trpy) OH$_2$)]$^{2+}$	0.56	0.19	11.2	[8]	[Ru^{II}(phen)([9]aneS$_3$)(Cl)]$^+$	1.15	[e]
[Ru^{II}(bpea)(bpy)(OH$_2$)]$^{2+}$	0.46	0.34	11.1	[1g]	[Ru^{II}(tpm)(phen)(Cl)]$^+$	0.67	[1f]
[Ru^{II}(trpy)(tmen)(OH$_2$)]$^{2+}$	0.59	0.36	10.8	[8]	[Ru^{II}(py)(phen)([9]aneS$_3$)]$^{2+}$	1.62	[17]
[Ru^{II}(tpm)(bpy)(OH$_2$)]$^{2+}$	0.71	0.40	10.8	[1f]	[Ru^{II}(tpm)(py)(bpy)]$^{2+}$	1.15	[24]
[Ru^{II}(tpm)(phen)(OH$_2$)]$^{2+}$	0.71	0.41	10.7	[1f]	[Ru^{II}(py)$_3$([9]aneS$_3$)]$^{2+}$	1.44	[25]
[Ru^{II}(trpy)(bpy)(OH$_2$)]$^{2+}$	0.62	0.49	9.7	[1a]	[Ru^{II}(tpm)(py)$_3$]$^{2+}$	1.02	[26]
[Ru^{II}([9]aneS$_3$)(phen)(OH$_2$)]$^{2+}$	–	0.77	10.2	[e]			
[Ru^{II}(trpy)(dppene)(OH$_2$)]$^{2+}$	1.53	1.17	–	[8]			

[a] Ligand abbreviations used: acac = acetylacetonate; dppene = *cis*-1,2-bis(diphenylphosphanyl)ethylene; tmen = *N*,*N*,*N*′,*N*′-tetramethylethylenediamine; bpea = *N*,*N*-bis(2-pyridyl)ethylamine. tpm = tris(1-pyrazolyl)methane. [b] Complexes in H$_2$O at pH = 7, μ = 0.1 phosphate buffer solution. [c] Redox potentials are reported with respect to the SSCE reference electrode. [d] Complexes in acetonitrile with 0.1 M tetraalkylammonium hexafluorophosphate. [e] This work.

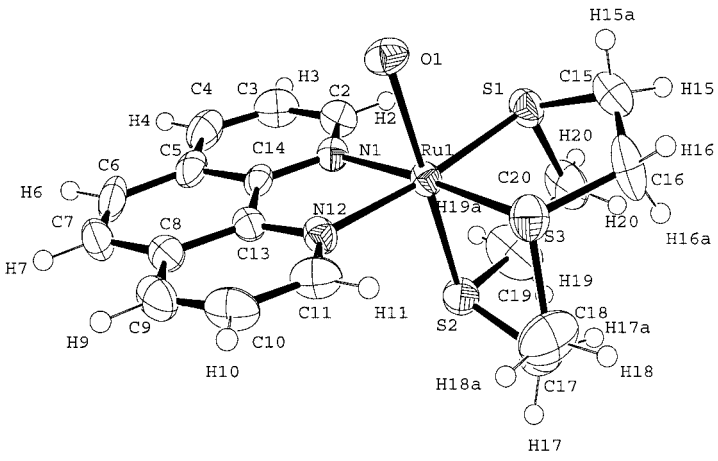

Figure 1. An ORTEP view (50% probability) of the molecular structure of cation **2**, including the atom labeling scheme

with no steric distortions from the other ligands.[13] In sharp contrast, the [9]aneS$_3$ ligand exerts a strong steric interaction over both the phen and the aqua ligands, which is clearly manifested, for instance, in the *trans* bonding angles that are all significantly smaller than 180°, ranging from 173.59(12)° to 177.54(10)°, thus producing a sort of umbrella folding [all *cis* X−Ru−S, X = N or O, angles are significantly larger than 90°, ranging from 91.03(10)° to 97.84(12)°, with a mean value for the six angles of 94.21(10)°]. Two disordered perchlorate anions balance the cationic charge. Finally, there are two waters of crystallization per complex that form an intricate network of hydrogen-bonds. O1w forms a strong hydrogen-bond with the aqua ligand bound to the Ru metal center and with the other crystallization water molecule (O2w). It also interacts weakly with one of the perchlorate counteranions. The other perchlorate ion interacts weakly with both the hydrogen atoms of the phen and the [9]aneS$_3$ ligands, whereas O2w interacts only with O1w and one of the perchlorate ions.

Spectroscopic Properties

The 1-D and 2-D NMR spectra for the aqua complex **2** were recorded in D_2O. The ^1H NMR spectrum of **2** is shown in Figure 2 (assignments are shown in the Exp. Sect.). The other NMR spectra are presented as supplementary information. All the resonances in the NMR spectra were unambiguously identified and are consistent with the same structure found in the solid-state. It is worth mentioning here that the cationic part of complex **2** is asymmetric. Nevertheless, from a magnetic point of view, at room temperature, it can be considered as having a plane of symmetry that bisects the [9]aneS$_3$ and the phen ligands in two halves, and which contains the Ru1, O1, and S2 atoms. The spectrum consists of a series of resonances in the δ = 2.4−3.6 ppm region that can be assigned to the thioether ligand, and a series of resonances in the δ = 5.8−9.6 ppm region arising from the phen ligand. There are three key NOESY effects together with the COSY map that allows for the unmistakable assignment of all the resonances observed in the ^1H NMR spectrum. The first two are interligand NOE effects observed between H11 (phen) and H17 (strong NOE effects, hydrogen atoms situated at a distance of 2.64 Å in the X-ray structure) and H18a (4.45 Å), which allows for the identification of the hydrogen atoms of the [9]aneS$_3$ ligand directed towards phen relative to those that are pointing away from the phen ligand. The third key NOE effect is also strong and is observed between H18 and H16a (2.47 Å), which allows for the clear differentiation of the H atoms of C17 from those of C18. Finally, the geminal protons can be assigned easily using the HETCOR ^1H-^{13}C map, and thus a complete assignment of the [9]aneS$_3$ ligand is achieved. With regard to the phen ligand, the resonances at δ = 7.95 and 8.15 ppm can be assigned to H10 and H7, respectively, based on their multiplicity. The doublet at 9.40 ppm is assigned to H11 based on the above-mentioned interligand NOE effects, and finally, the doublet at δ = 8.67 ppm is assigned to H9. The assignments for the phen ligand are consistent with the COSY map.

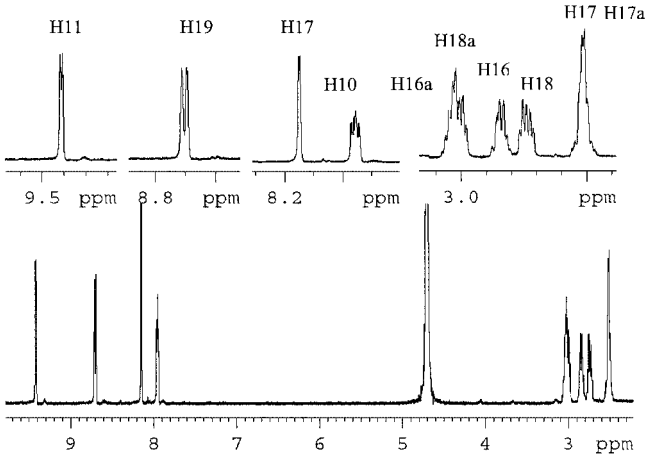

Figure 2. ^1H NMR spectrum of the complex **2** recorded in D_2O; amplifications of selected zones are displayed on top

The electronic spectrum of the aqua complex **2** at pH 7.0 is shown in Figure 3. Below 300 nm two predominantly ligand based $\pi-\pi^*$ transitions appear at λ_{max} = 259 nm (ε = 39750 $cm^{-1}M^{-1}$) and 288 nm (15355 $cm^{-1}M^{-1}$); above 300 nm two bands appear at 353 nm (6766 $cm^{-1}M^{-1}$) and 410 nm (6578 $cm^{-1}M^{-1}$) that can be assigned to a series of MLCT $d\pi-\pi^*$(Ru−phen) transitions and their vibronic components, based on previous literature for related complexes.[1g,11,14] Under basic conditions complex **2** deprotonates generating the corresponding hydroxy derivative, $[Ru^{II}(OH)(phen)([9]aneS_3)]^+$ (**3**). For the hydroxo complex **3**, the two MLCT bands are shifted to higher wavelengths relative to those of the corresponding Ru−aqua complex **2** [410 nm (6816 $cm^{-1}M^{-1}$) and 432 nm (6811 $cm^{-1}M^{-1}$)] due to the relative destabilization of $d\pi$ (Ru) levels prompted by the hydroxo ligand.[1g,15] A pK_a of 10.1 is obtained from the acid-base spectrophotometric titration of **2** (shown as an inset in Figure 3), giving one isosbestic point at 379 nm, see Equation (4).

$$[Ru^{II}(phen)(H_2O)(9aneS_3)]^{2+} \longrightarrow [Ru^{II}(OH)(phen)(9aneS_3)]^{+} + H^{+} \quad (4)$$

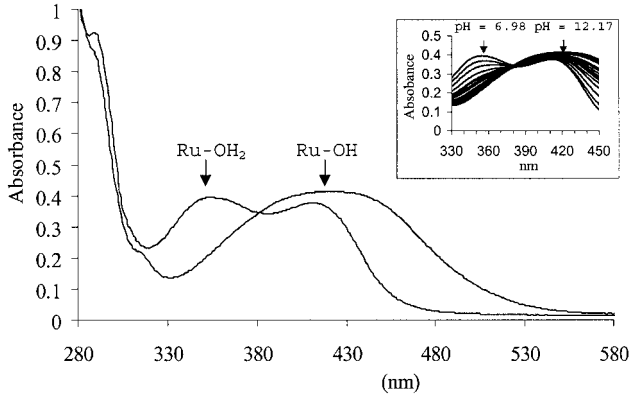

Figure 3. UV/Vis spectra of complex **2** at pH 7.0 phosphate buffer, and of complex **3** at pH 12.2. The inset shows the acid-base spectrophotometric titration of a $5\cdot10^{-5}$ M solution of **2** in the 330−450 nm region (the pH of the different spectra are 7.0, 9.2, 9.6, 9.9, 10.15, 10.3, 10.5, 10.7, 11.2, 11.3, 11.7, 10.05, 12.2)

Redox Chemistry and Catalytic Properties

The redox properties of the aqua complex **2** were investigated by means of cyclic voltammetric and coulometric techniques. Figure 4 shows the cyclic voltammograms of complex **2** at pH = 7.0, in the presence and absence of benzyl alcohol, BzOH, and their mathematical simulation has been performed using the software DIGISIM and is presented as Supporting Information.[16] As can be observed, a chemically irreversible wave is obtained at pH = 7.0 and at a scan rate of 100 mV/s, with $E_{p,a}$ = 0.82 V and a small returning wave at $E_{p,c}$ = 0.72 V ($E_{1/2}$ = 0.77 V; ΔE = 100 mV); these redox processes have been tentatively assigned to the Ru^{III}/Ru^{II} redox couple based on electronic arguments (vide infra) and whilst taking into consideration that the charge under the anodic wave is similar to that of the Ru^{III}/Ru^{II} couple of $[Ru^{II}(py)(phen)([9]aneS_3)]^{2+}$ [17] which behaves in a reversible manner. No further electrochemical processes are observed under these conditions for potentials up to 1.7 V. In sharp contrast, the homologous Ru−Cl complex **1**, displays a reversible wave due to the Ru^{III}/Ru^{II} couple with $E_{1/2}$ = 1.15 V ($E_{p,a}$ = 1.19 V, $E_{p,c}$ = 1.11 V, ΔE = 81 mV), in acetonitrile. For the Ru−OH_2 complex, **2**, the reduction potential observed varies with pH with a slope of 56.0 mV per pH unit, as expected for this type of compound. The corresponding Pourbaix diagram in the pH range from 6 to 10 is shown as supplementary information. Several attempts have been undertaken to further characterize the Ru^{III}/Ru^{II} couple by performing CV experiments at different temperatures and at different scan rates, but the results did not give further meaningful information. The instability of the Ru^{III}−OH species manifested in the CV is also displayed when it is oxidized using NaOCl as the oxidant at pH = 2.5, as expected. The process was followed spectrophotometrically and is shown as supplementary material. In the UV/Vis spectrum the initial bands of **2** at 353 and 410 nm progressively disappear on addition of NaOCl, generating a spectrum with new bands of low intensity at 320 and 370 nm, with two isosbestic points at 280 and 330 nm. Given this chemically irreversible behavior two possibilities arise: the formation of a μ-oxo species or disproportionation to Ru^{II} and Ru^{IV}, followed by the oxidation of the $[9]aneS_3$ ligand to the corresponding sulfoxide. The former is ruled out since Ru−O−Ru species have a very characteristic band in the 550−650 nm range[18] that is not observed in the present case, whereas strong evidence for the latter is obtained. The addition of NaOCl to **2** was also followed by NMR spectroscopy. A shift to lower field is observed for the signals of all the methylenic protons of $[9]aneS_3$, in agreement with the oxidation to their corresponding sulfoxide species. This statement is also supported by the fact that no electroactivity of the oxidized species is observed in the 0.0−1.2 V potential window at pH = 7.0, due to the strong electron-withdrawing capacity of the sulfoxide species which prevents further oxidations of the newly generated diamagnetic Ru^{II} complex.

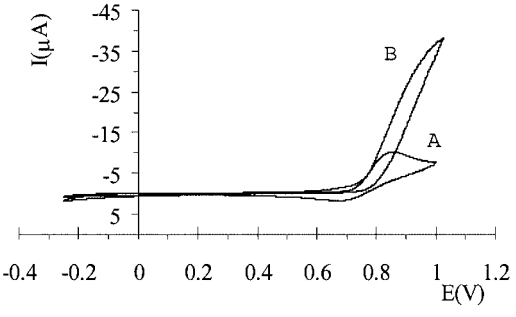

Figure 4. Cyclic voltammograms at a scan rate of 20 mV/s of complex **2** at pH = 7.0 in the absence (A) and presence of 0.2 M BzOH (B)

Table 3 presents the pK_a and electrochemical information of several polypyridylic Ru−Cl, Ru−OH_2, and Ru−py (py = pyridine). As can be seen, the redox properties of the Ru−H_2O type of complexes are highly sensitive to the nature of the ancillary ligands. Strong σ-electron donors stabilize the Ru^{III} oxidation state and thus a decrease in the Ru^{III}/Ru^{II} reduction potential is observed. The opposite effect is observed with good π-electron acceptor ligands which increase the Ru^{III}/Ru^{II} redox potential due to the stabilization of Ru^{II} by dπ−π* back-bonding.[10]

For **2**, comparison of the redox potentials can be made with $[Ru(tpm)(N\text{-}N)(L)]^{2+}$ (tpm, tris(1-pyrazolyl)methane; N-N is bpy or phen; L = H_2O, Cl, or py). The tpm complexes are a convenient choice since, like [9]aneS_3, tpm is a tridentate facial ligand, and therefore the influence of geometrical aspects on redox potentials is minimized. Thus, when comparing the Ru^{III}/Ru^{II} redox potential of the aqua complexes, $[Ru(T)(N\text{-}N)(H_2O)]^{2+}$ (T = tpm or [9]aneS_3), it is found that the thioether ligand produces an increase of 360 mV with regard to the corresponding tpm complex, due to both a much weaker σ-donor capacity and a stronger π-acceptor ability of the former ligand.[19] A similar phenomenon is also found for the Ru−Cl and Ru−py complexes where, as shown in Table 3, an increase of 480 and 420−470 mV in the Ru^{III}/Ru^{II} redox potential is observed, respectively.

The combination of σ- and π-electronic perturbations exerted by the [9]aneS_3 ligand over the ruthenium metal center results in an increase in the Ru^{III}/Ru^{II} redox potential for the Ru−aqua complex **2**, that in turn is responsible for the instability of the corresponding Ru^{III}−OH species, which undergoes a decomposition process. This increase in the redox potentials is also manifested by the fact that the corresponding Ru^{IV}/Ru^{III} redox wave is not found throughout the entire pH range, on scanning up to 1.7 V. The high reactivity of the Ru^{III}−OH species is also shown by its ability to oxidize BzOH. This is illustrated in Figure 4, where the cyclic voltammograms are recorded both in the presence and absence of BzOH. When the alcohol is present, there is a strong enhancement of the anodic peak current due to the electrocatalytic oxidation of the alcohol forming benzaldehyde.[20] Meyer and co-workers[20b] have previously proposed a Ru^{III}−OH species that is capable of oxidizing BzOH, even though it is usually the Ru^{IV} species that is capable of carrying out such an oxidation reaction. In our study, the strong electron-withdrawing nature of the [9]aneS_3 ligand results in a high increase in the Ru^{III}/Ru^{II} redox potential, and thus it is plausible that the +3 oxidation state is sufficiently reactive so as to oxidize BzOH.

Increasing amounts of BzOH (0.10, 0.18, 0.20 M) were added to the solution and a series of cyclic voltammograms were recorded with a scan rate of 20 mV/s (see Figure 4 and the Supplementary Information). At this scan rate, the system behaves in a steady-state condition, and thus the limiting current is predicted to be independent of scan rate.[21] A second-order rate constant, k_{cat} = 19.3 $M^{-1}s^{-1}$, is experimentally determined using the equation described by Shain et al.[21] A similar value is also obtained, k_{cat} = 19.8 $M^{-1}s^{-1}$, from the mathematical simulation (See supplementary material) of the process using DIGISIM. This value is of the same order of magnitude as for the polypyridylic Ru^{IV}=O complexes described previously in the literature,[22] which are capable of oxidizing the same substrate under similar conditions, with k_{cat} values ranging from 6.0 to 30.8 $M^{-1}s^{-1}$. The formation of benzaldehyde as the only product was corroborated in a bulk experiment using the following conditions: 1.46 mM **2**/0.145 M BzOH/$9.09\cdot10^{-3}$ M NaOCl/pH 6.9 phosphate. This system yields 8.55 mM benzaldehyde after 15 minutes at 22.0 °C.

In summary, a new Ru−aqua complex, **2**, containing the soft [9]aneS_3 ligand has been prepared and its structural, spectroscopic and redox properties are described. The bonding of the facial thioether ligand by the Ru metal center results in a high anodic shift of the Ru^{III}/Ru^{II} couple relative to the complex $[Ru(tpm)(phen)(H_2O)]^{2+}$, due to the weaker σ- and stronger π-bonding capacities exerted by [9]aneS_3 over the Ru metal center relative to the pyrazolylic ligand. These electronic interactions are also responsible for the instability of the corresponding Ru^{III}−OH species. However, the decomposition reaction coupled to the Ru^{III}−OH species is slower than the oxidation of BzOH that yields the initial Ru^{II}−OH_2 and benzaldehyde, thus generating a catalytic cycle.

Experimental Section

Materials: All reagents used in the present work were obtained from Aldrich Chemical Co and were used without further purification. Reagent grade organic solvents were obtained from SDS, and high purity deionized water was obtained by passing distilled water through a nanopure Mili-Q water purification system. The complex $[Ru^{II}(Cl)(phen)([9]aneS_3)]Cl$, **1**, was prepared according to literature procedures and recrystallized twice from methanol prior to its use.[11]

Preparations: All synthetic manipulations were routinely performed under a nitrogen atmosphere using Schlenk tubes and vacuum line techniques in the dark. Electrochemical experiments were performed in the dark under a N_2 or Ar atmosphere with degassed solvents.

Caution! The complex described in this section contains the perchlorate ion as a counteranion; perchlorate salts are potentially explosive.

$[Ru^{II}(phen)(OH_2)([9]aneS_3)](ClO_4)_2\cdot2H_2O$ (2·2H_2O): A sample of **1** (35 mg, 0.051 mmol) was added to a solution of $AgClO_4$ (27.0 mg, 0.130 mmol) dissolved in water/acetone (1:1) (15 mL). The resulting mixture was refluxed for 2 h. AgCl was filtered through a frit containing celite and the volume was reduced using a rotary evaporator under reduced pressure until the solution started to become turbid. A pale orange solid the precipitated. The solid was washed with hexane and diethyl ether and dried under vacuum. Yield: 23.5 mg (53%). $C_{18}H_{22}Cl_2N_2O_9RuS_3\cdot2H_2O$: found (calcd.) C 30.47 (30.25), H 3.72 (3.64), N 4.03 (3.92), S 13.30 (13.44). ^{1}H NMR (500 MHz, D_2O, 25 °C): δ, 2.50 (m, H17, H17a), 2.75 (m, H18), 2.85 (m, H16), 3.00 (m, H18a), 3.05 (m, H16a), 7.95 (dd, J_{9-10} = 7.7, J_{10-11} = 3.8 Hz, H10), 8.15 (d, J_{7-9} = 0.5 Hz, H7), 8.67 (d, J_{9-10} = 7.7 Hz, H9), 9.40 (d, J_{11-10} = 3.8 Hz, H11) ppm. ^{13}C NMR (500 MHz,

D_2O, 25 °C): δ, 32.5 (C18), 33.02 (C16), 35.07 (C17), 127.34 (C10), 129.07 (C7), 132.2 (C8), 139.8 (C9), 148 (C13), 155.1 (C11). For the NMR spectroscopic assignments we have used the same labeling scheme as those used in the X-ray structure shown in Figure 1. $E_{1/2}$ (pH, 7.0 phosphate buffer) = 0.77 V vs. SSCE. UV/Vis (pH, 7.0 phosphate buffer) $\lambda_{max,}$ nm (ε, $M^{-1}cm^{-1}$), assignment: 259 (39750) π−π*; 288 (15355) π−π*; 353 (6766) dπ−π*(phen); 410 (6578) dπ−π*(phen).

Instrumentation and Measurements: UV/Vis spectroscopy was performed on a Cary 50 Scan (Varian) UV/Vis spectrophotometer using 1 cm quartz cells. pH measurements were performed using a Micro-pH-2000 instrument from Crison. Cyclic voltammetric (CV) experiments were performed with a PAR 263A EG&G potentiostat or an IJ-Cambria IH-660 using a three electrode cell. A glassy carbon disc electrode (3 mm diameter) from BAS was used as the working electrode, platinum wire as auxiliary and SSCE as the reference electrode. All cyclic voltammograms presented in this work were recorded under a nitrogen atmosphere. The pH was adjusted from 0−2 with HCl, adding sodium chloride to keep a minimum ionic strength of 0.1 M. From pH 2−10, 0.1 M phosphate buffers were used, and from pH 10−12 diluted CO_2 free NaOH was used. All $E_{1/2}$ values reported in this work were estimated from cyclic voltammetry as the average of the oxidation and reduction peak potentials $(E_{p,a} + E_{p,c})/2$. Unless explicitly mentioned, the concentrations of the complexes were approximately 1 mM.

Catalytic studies at neutral pH have been performed in phosphate buffer solution. The conversion of benzyl alcohol to benzaldehyde was followed by GC using Shimadzu GC-17A gas chromatography apparatus in a TRA-5 Column (30 m × 0.25 mm diameter) incorporating a FID detector. GC conditions: initial temperature 80 °C for 1 min, ramp rate 10 °/min, final temperature 220 °C, injection temperature 220 °C, detector temperature 250 °C, carrier gas He at 25 mL/min. Under these conditions, the retention times for benzaldehyde and benzyl alcohol are 3.9 and 4.9 minutes, respectively.

NMR spectroscopy was performed on a Bruker 500 MHz or a Bruker DPX 200 MHz spectrometer. Samples were run in deuterium oxide. Elemental analyses were performed using a CHNS-O Elemental Analyser EA-1108 from Fisons.

X-ray Structure Determination: Suitable crystals of $[Ru(phen)(H_2O)([9]aneS_3)](ClO_4)_2{\cdot}2H_2O$ (**2·2H$_2$O**) were grown from water as yellow blocks. A prismatic crystal (0.1 × 0.1 × 0.2 mm) was selected and mounted on an Enraf−Nonius CAD4 four-circle diffractometer. Unit-cell parameters were determined from automatic centering of 25 reflections ($12 < \theta < 21°$) and refined by least-squares methods. Intensities were collected with graphite monochromatized Mo-*Kα* radiation, using the ω/2θ scan-technique. 7668 reflections were measured in the range $2.21 \leq \theta \leq 29.97°$, of which 7617 were independent ($R_{int} = 0.010$), and 3557 reflections were assumed as observed applying the condition $I > 2\sigma(I)$. Three reflections were measured every two hours as orientation and intensity controls, significant intensity decay was not observed. Lorentz-polarization but no absorption corrections were made.

The structure was solved by Patterson synthesis, using the SHELXS computer program[23a] and refined by full-matrix least-squares methods with the SHELXL-97 computer program[23a], using 7617 reflections. The function minimized was $\Sigma w\|F_o|^2 + |F_c|^2|^2$, where $w = [\sigma^2(I) + (0.0440P)^2]^{-1}$ and $P = (F_o^2 + 2F_c^2)/3$; f, f′, and f″ were taken from International Tables of X-ray Crystallography.[23b] All H atoms were computed and refined, using a riding model, with an isotropic temperature factor equal to 1.2 times the equivalent of the temperature factor of the atoms which are linked. The final R (on F) factor was 0.0386, wR (on F^2) = 0.0580 and the goodness of fit was 0.845 for all observed reflections. The number of refined parameters was 298. Max. shift/esd = 0.014, mean shift/esd = 0.002. Max. and min. peaks in the final difference synthesis was 0.538 and −0.677 $e{\cdot}Å^{-3}$, respectively.

Crystallographic data for the structure included in this paper have been deposited with the Cambridge Crystallographic Data Centre as supplementary publication no. CCDC-204307. These data can be obtained free of charge at http://www.ccdc.cam.ac.uk/conts/retrieving.html [or from the Cambridge Crystallographic Data Centre, 12 Union Road, Cambridge CB2 1EZ, UK; Fax: (internat.) +44-1223-336-033; E-mail: deposit@ccdc.cam.ac.uk].

Acknowledgments

This research has been financed by MCYT of Spain through project BQU2000−0458. AL is grateful to CIRIT Generalitat de Catalunya (Spain) for the Distinction award and the aid SGR2001-UG-291. AL also thanks Johnson and Matthey for a $RuCl_3{\cdot}xH_2O$ loan. X.S and A.P are grateful for the award of a doctoral grant from the University of Girona and from CIRIT, respectively.

[1] [1a] R. A. Binstead, T. J. Meyer, *J. Am. Chem. Soc.* **1987**, *109*, 3287. [1b] C. M. Che, T. F. Lai, K. Y. Wong, *Inorg. Chem.* **1987**, *26*, 2289. [1c] J. H. Muller, J. H. Acquaye, K. J. Takeuchi, *Inorg. Chem.* **1992**, *31*, 4552. [1d] A. Gerli, J. Reedijk, M. T. Lakin, A. L. Spek, *Inorg. Chem.* **1995**, *34*, 1836. [1e] X. Hua, M. Shang, A. G. Lappin, *Inorg. Chem.* **1997**, *36*, 3735. [1f] A. Llobet, P. Doppelt, T. J. Meyer, *Inorg. Chem.* **1998**, *27*, 514. [1g] M. Rodriguez, I. Romero, A. Llobet, A. Deronzier, M. Biner, T. Parella, H. Stoeckli-Evans, *Inorg. Chem.* **2001**, *40*, 4150. [1h] M. Shiotsuki, H. Miyai, Y. Ura, T. Suzuki, T. Kondo, T. Mitsudo, *Organometallics* **2002**, *21*, 4960. [1i] M. H. V. Huynh, L. M. Witham, J. M. Lasker, M. Wetzler, B. Mort, D. L. Jameson, P. S. White, K. J. Takeuchi, *J. Am. Chem. Soc.* **2003**, *125*, 308.

[2] [2a] J. C. Dobson, W. K. Seok, T. J. Meyer, *Inorg. Chem.* **1986**, *25*, 1513. [2b] A. S. Goldstein, R. H. Beer, R. S. Drago, *J. Am. Chem. Soc.* **1994**, *116*, 2424. [2c] L. K. Stultz, R. A. Binstead, M. S. Reynolds, T. J. Meyer, *J. Am. Chem. Soc.* **1995**, *117*, 2520. [2d] W. C. Cheng, W. Y. Yu, K. K. Cheung, S. M. Peng, C. K. Poon, C. M. Che, *Inorg. Chim. Acta* **1996**, *242*, 105. [2e] C. Ho, C. M. Che, T. C. Lau, *J. Chem. Soc., Dalton Trans.* **1990**, 967. [2f] D. Carmona, C. Cativiela, S. Elipe, F. J. Lahoz, M. P. Lamata, M. Pilar, M. L. R. Deviu, L. A. Oro, C. Vega, F. Viguri, *Chem. Commun.* **1997**, 2351. [2g] W. H. Fung, W. Y. Yu, C.-M. Che, *J. Org. Chem.* **1998**, *63*, 7715.

[3] [3a] L. Roecker, J. C. Dobson, W. J. Vining, T. J. Meyer, *Inorg. Chem.* **1987**, *26*, 779. [3b] J. H. Acquaye, J. G. Muller, K. J. Takeuchi, *Inorg. Chem.* **1993**, *32*, 160. [3c] X. Hua, A. G. Lappin, *Inorg. Chem.* **1995**, *34*, 992. [3d] L. F. Szczepura, S. M. Maricich, R. F. See, M. R. Churchill, K. J. Takeuchi, *Inorg. Chem.* **1995**, *34*, 4198. [3e] X. Hua, M. Shang, A. G. Lappin, *Inorg. Chem.* **1997**, *36*, 3735.

[4] [4a] B. A. Moyer, B. K. Sipe, T. J. Meyer, *Inorg. Chem.* **1981**, *20*, 1475. [4b] W. K. Seok, Y. J. Son, S. W. Moon, H. N. B. Lee, *Kor. Chem. Soc.* **1998**, *19*, 1084.

[5] [5a] M. S. Thompson, T. J. Meyer, *J. Am. Chem. Soc.* **1982**, *104*, 4106. [5b] L. E. Roecker, T. J. Meyer, *J. Am. Chem. Soc.* **1987**, *109*, 746. [5c] M. E. Marmion, K. J. Takeuchi, *J. Am. Chem. Soc.* **1988**, *110*, 1742. [5d] R. A. Binstead, M. E. MacGuire, A. Dovletoglou, W. K. Seok, L. E. Roecker, T. J. Meyer, *J. Am. Chem. Soc.* **1992**, *114*, 173. [5e] C. M. Che, C. Ho, T. C. Lau, *J. Chem. Soc., Dalton Trans.* **1991**, 1259. [5f] V. J. Catalano, R. A. Heck, C. E. Immoos, A. Ohman, M. G. Hill, *Inorg. Chem.*

1998, *37*, 2150. [5g] C. M. Che, K. W. Cheng, M. C. W. Chan, T. C. Lau, C. K. Mak, *J. Org. Chem.* **2000**, *65*, 7996−8000.

[6] [6a] T. C. Lau, C. M. Che, W. O. Lee, C. K. Poonl, *J. Chem. Soc., Chem. Commun.* **1988**, 1406. [6b] C. M. Che, V. W. W. Yam, T. C. W. Mak, *J. Am. Chem. Soc.* **1990**, *112*, 2284. [6c] N. Grover, S. A. Ciftan, H. H. Thorp, *Inorg. Chim. Acta* **1995**, *240*, 335. [6d] C. Morice, P. Lemaux, C. Moinet, G. Simonneaux, *Inorg. Chim. Acta* **1998**, *273*, 142. [6e] K. Jitsukawa, Y. Oka, H. Einaga, H. Masuda, *Tetrahedron Letters* **2001**, *42*, 3467.

[7] [7a] A. H. Krotz, L. Y. Kuo, J. K. Barton, *Inorg. Chem.* **1993**, *32*, 5963. [7b] T. M. Santos, B. J. Goodfellow, M. G. B. Drew, J. Pedrosa de Jesus, V. Félix, *Metal Based Drugs* **2001**, *8(3)*, 125. [7c] S. Delaney, M. Pascaly, P. K. Bhattacharya, J. K. Barton, *Inorg. Chem.* **2002**, *41*, 1966. [7d] O. Schiemann, J. K. Barton, N. J. Turro, *J. Phys. Chem. B* **2000**, *104*, 7214.

[8] A. Dovletoglou, S. Ajao Adeyemi, T. J. Meyer, *Inorg. Chem.* **1996**, *35*, 4120.

[9] A. Llobet, *Inorg. Chim. Acta* **1994**, *221*, 125.

[10] [10a] R. A. Leising, K. J. Takeuchi, *Inorg. Chem.* **1987**, *26*, 4391. [10b] C. A. Bessel, R. A. Leising, K. J. Takeuchi, *J. Chem. Soc., Chem. Commun.* **1991**, 883.

[11] B. J. Goodfellow, V. Félix, S. M. Pacheco, J. Pedrosa de Jesus, M. G. B. Drew, *Polyhedron* **1997**, *16*, 393.

[12] [12a] C. Landgrafe, W. S. Sheldrick, *J. Chem. Soc., Dalton Trans.* **1994**, 1885. [12b] B. J. Goodfellow, S. M. Pacheco, J. Pedrosa de Jesus, V. Félix, M. G. B. Drew, *Polyhedron* **1997**, *16*, 3293. [12c] T. M. Santos, B. J. Goodfellow, J. Madureira, J. Pedrosa de Jesus, V. Félix, M. G. B. Drew, *New J. Chem.* **1999**, *23*, 1015. [12d] J. Madureira, T. M. Santos, B. J. Goodfellow, M. Lucena, J. Pedrosa de Jesus, M. G. Santana-Marques, M. G. B. Drew, V. Félix, *J. Chem. Soc., Dalton Trans.* **2000**, 4422.

[13] G. J. Grant, S. S. Shoup, C. L. Baucom, W. N. Setzer, *Inorg. Chim. Acta* **2001**, *317*, 91.

[14] [14a] J. Z. Wu, B. H. Ye, L. Wang, L. N. Ji, J. Y. Zhou, R. H. Li, Z. Y. Zhou, *J. Chem. Soc., Dalton Trans.* **1997**, 1395. [14b] B. J. Coe, S. Hayat, R. L. Bedoes, M. Helliwell, J. C. Jeffrey, S. R. Batten, P. S. White, *Dalton Trans.* **1997**, 591.

[15] K. J. Takeuchi, H. S. Thompson, D. W. Pipes, T. J. Meyer, *Inorg. Chem.* **1984**, *23*, 1845.

[16] DigiSim for Windows 95. Version 3.05. File type: CV. Bioanalytical Systems.

[17] X. Sala, I. Romero, M. Rodríguez, A. Llobet, unpublished work.

[18] [18a] A. Llobet, M. E. Curry, H. T. Evans, T. J. Meyer, *Inorg. Chem.* **1989**, *28*, 3131. [18b] T. R. Weaver, T. J. Meyer, S. A. Adeyemi, G. M. Brown, R. P. Eckberg, W. E. Hatfield, R. W. Murray, D. J. Untereker, *J. Am. Chem. Soc.* **1975**, *97*, 3039.

[19] [19a] G. J. Grant, T. Salupobryant, L. A. Holt, D. Y. Morrissey, M. J. Gray, J. D. Zubkowski, E. J. Valente, L. F. Mehne, *J. Organomet. Chem.* **1999**, *587*, 207. [19b] S. R. Cooper, *Acc. Chem. Res.* **1988**, *21*, 141.

[20] [20a] T. J. Meyer, *J. Electrochem. Soc.* **1984**, *131*, 221C. [20b] L. K. Stultz, M. H. V. Huynh, R. A. Binstead, M. Curry, T. J. Meyer, *J. Am. Chem. Soc.* **2000**, *122*, 5984.

[21] Under steady-state conditions, the limiting current is predicted to be independent of scan rate, and the second-order rate constant is given by the expression, $i_L = n{\cdot}F{\cdot}A{\cdot}C_o{\cdot}(D{\cdot}k_{cat}{\cdot}C_s)^{1/2}$ where i_L is the limiting current, n is the number of electrons transferred, A is the electrode area, C_o is the concentration of Ru^{II}, D is the diffusion coefficient, and C_s is the substrate concentration. [21a] D. S. Polcyn, I. Shain, *Anal. Chem.* **1966**, *38*, 376. [21b] A. J. Bard, L. R. Faulkner, in: *Electrochemical Methods; Wiley*; New York, **1980**.

[22] [22a] V. J. Catalano, R. A. Heck, C. E. Immoos, A. Ohman, M. Hill, *Inorg. Chem.* **1998**, *37*, 2150. [22b] E. L. Lebeau, T. J. Meyer, *Inorg. Chem.* **1999**, *38*, 2174. [22c] A. Gerli, J. Reedijk, M. T. Lakin, A. L. Spek, *Inorg. Chem.* **1995**, *34*, 1836.

[23] [23a] G. M. Sheldrick, **1997**. Univer. Göttingen, Germany. [23b] International Tables of X-ray Crystallography, **1974**, Ed. Kynoch Press, vol. IV, pp. 99−100 and 149.

[24] K. Barkawi, A. Llobet, T. J. Meyer, *J. Am. Chem. Soc.* **1988**, *110*, 7751.

[25] S. Roche, H. Adams, S. E. Spey, J. A. Thomas, *Inorg. Chem.* **2000**, *39*, 2385.

[26] F. Laurent, E. Plantalech, B. Donnadieu, A. Jimenez, F. Hernandez, M. Martinez-Ripoll, M. Biner, A. Llobet, *Polyhedron* **1999**, *18*, 3321.

Received March 13, 2003
Early View Article
Published Online December 4, 2003

